NASA CONTRACTOR REPORT

NASA CR-2326

NASA CR-2326

A NON-COHERENT MODEL FOR MICROWAVE EMISSIONS AND BACKSCATTERING FROM THE SEA SURFACE

by S. T. Wu and A. K. Fung

Prepared by
THE UNIVERSITY OF KANSAS CENTER FOR RESEARCH, INC.
Lawrence, Kans. 66044
for Langley Research Center

NATIONAL AERONAUTICS AND SPACE ADMINISTRATION • WASHINGTON, D. C. • NOVEMBER 1973

1. Report No.	2. Government Accession No.	3. Recipient's Catalog No.
NASA CR-2326		

4. Title and Subtitle	5. Report Date
A Non-Coherent Model for Microwave Emissions and Backscattering From the Sea Surface	November 1973
	6. Performing Organization Code
7. Author(s)	8. Performing Organization Report No.
S. T. Wu and A. K. Fung	Technical Report 186-3
9. Performing Organization Name and Address	10. Work Unit No.
University of Kansas Center For Research, Inc. 2291 Irving Hill Road - Campus West Lawrence, Kansas 66044	11. Contract or Grant No. NAS 1-10048
	13. Type of Report and Period Covered
12. Sponsoring Agency Name and Address	Contractor Report
National Aeronautics and Space Administration Washington, D. C. 20546	14. Sponsoring Agency Code

15. Supplementary Notes

This is a topical report.

16. Abstract

The two-scale (small irregularities superimposed upon large undulations) scattering theory proposed by Semyonov has been extended and used to compute microwave apparent temperature and the backscattering cross section from ocean surfaces. The effect of the small irregularities upon the scattering characteristics of the large undulations is included by modifying the Fresnel reflection coefficients; whereas the effect of the large undulations upon those of the small irregularities is taken into account by averaging over the surface normals of the large undulations.

The same set of surface parameters is employed for a given wind speed to predict both the scattering and the emission characteristics at both polarizations. Improved agreement with measured results is demonstrated when compared with predictions by a single scale surface. This indicates that the sea surface is better modeled by a composite rather than a single surface. The results also imply that the adequacy of a scattering model is best exemplified when it is used to predict both the scattering and the emission characteristics.

17. Key Words (Selected by Author(s))	18. Distribution Statement
Non-coherent model Microwave emission and backscattering Two-scale sea surface Agreement with measurements	Unclassified - Unlimited

19. Security Classif. (of this report)	20. Security Classif. (of this page)	21. No. of Pages	22. Price*
Unclassified	Unclassified	34	Domestic, $3.00 Foreign, $5.50

*For sale by the National Technical Information Service, Springfield, Virginia 22151

FOREWORD

The value of microwave scatterometers and radiometers as remote sea wind sensors has been independently demonstrated by a number of investigators. However, near-simultaneous observations by a composite radiometer and scatterometer (RADSCAT) instrument have been judged to have value in making better estimates of the surface winds beyond the improvement provided by two independent measurements. To demonstrate this potential a joint effort between New York University, General Electric Space Division , the University of Kansas and NASA Langley Research was undertaken through the Advanced Applications Flight Experiment program of NASA. This document reports the investigations performed by the University of Kansas during the first year of this joint program.

Specifically, this report was prepared by the Remote Sensing Laboratory of the University of Kansas Center for Research, Inc., under Contract NAS 1-10048.

TABLE OF CONTENTS

I. INTRODUCTION

The microwave emission characteristic of the sea has been measured by several investigators [1,2,3,4,5]. These investigators have compared their observations with predictions from geometric optics theory [6] which uses a single surface model and found some but not satisfactory agreement between predictions and measurements. The wind dependence of the geometric optics approach was based on measured rms sea slope data presented by Cox and Munk [7]. However, the theory failed to predict the observed emission characteristics near nadir and fitted only loosely for nadir angles between 30 and 70 degrees. The failure of the geometric optics model to account for wind dependence at nadir was first reported by Nordberg, et al. [1], and verified by Hollinger [5].

In view of the above deficiencies, an investigation is necessary to seek a more adequate model for microwave emissions from the sea. The emphasis in this investigation is oriented towards using a composite surface model which better reflects the roughness characteristic of the sea. Since several lengthy numerical integrations are required to yield the emissivity, the more adequate model must not be so complicated as to make numerical calculations prohibitive. With this perspective, a non-coherent scattering theory of the type described by Semyonov [8] is extended to yield the bistatic scattering coefficient. Since an acceptable scattering coefficient for predicting the microwave emission characteristics must also be acceptable for predicting backscattering, the latter case is examined to provide a cross check on the model.

To compare with experimental observations, an isotropic surface characteristic, although not realistic for the ocean surface, is assumed. A justification for this assumption is based on the observed directional insensitivity of emissions from the sea [9]. The two-scale rough surface model is also assumed to have Gaussian surface height distribution and Gaussian surface correlation for both scales. The dielectric constant needed in the calculations is based on the data reported by Saxton and Lane [10].

The wind dependence of the surface parameters in the composite model is introduced in accordance with rms slope data measured by Cox and Munk for the large undulations and Sutherland's [11] results for the small irregularities. Details

for the theory and the choice of surface parameters are given in sections II and III respectively. Comparisons of the computed brightness temperature and backscattering characteristics at two different wind speeds are made with both measured data and the predictions of a single surface model. The results are presented in section IV.

II. A SURFACE BRIGHTNESS TEMPERATURE THEORY

II.1 Formulation of the Problem

The basic theory of surface brightness temperature was developed by Peake [12]. The relationship among the surface emissivity, the surface temperature and the brightness temperature is as follows:

$$T_{Bj}(\theta)=\epsilon_j(\theta)\,T_g \qquad j = h \text{ or } v$$

where $T_{Bj}(\theta)$ is the brightness temperature; $\epsilon_j(\theta)$ the emissivity; T_g the surface temperature; h denotes horizontal polarization and v vertical polarization. Note that the azimuthal angle ϕ needed together with the nadir angle θ to specify a direction has been chosen to be zero without loss of generality.

The connection between the emissivity and the differential scattering coefficient of the surface, $\gamma_j(\theta,\theta_s,\phi_s)$ is

$$\epsilon_j(\theta) = 1-\frac{1}{4\pi}\int_0^{2\pi}\int_0^{\frac{\pi}{2}} \gamma_j(\theta,\theta_s,\phi_s)\sin\theta_s\, d\theta_s\, d\phi_s \qquad (1)$$

where θ_s, ϕ_s are angles defining the direction of scattering corresponding to a wave incident at an angle θ.

The basic formulation of the problem indicated above shows that the differential scattering coefficient is the quantity that defines the angular characteristics of the brightness temperature of a given surface. Consequently, different brightness temperature theories are also distinguished by the different models assumed for the differential scattering coefficient.

Under the non-coherent assumption $\gamma_j(\theta,\theta_s,\phi_s)$ can be shown [8] to consist of two terms, i.e.

$$\gamma_j(\theta,\theta_s,\phi_s) = \gamma_j^{\circ}(\theta,\theta_s,\phi_s) + \langle \gamma_j^{1}(\theta,\theta_s,\phi_s)\rangle \qquad (2)$$

where $\gamma_j^{\circ}(\theta,\theta_s,\phi_s)$ denotes the main contribution by the large undulations; $\langle\gamma_j^{1}(\theta,\theta_s,\phi_s)\rangle$ denotes the differential scattering coefficient of the small irregularities averaged over the distribution of the surface normals of the large undulations. Detailed derivations for $\gamma_j^{\circ}(\theta,\theta_s,\phi_s)$ and $\langle\gamma_j^{1}(\theta,\theta_s,\phi_s)\rangle$ are given in sections II.2 and II.3 respectively.

Since the backscattering cross-section is a special case of the differential scattering coefficients, it can be obtained from the known differential scattering coefficients, (see Figure 1) i.e.

$$\sigma^{\circ}_{Bj}(\theta) = \cos\theta \cdot \gamma_j(\theta, \theta_s, \phi_s)\Big|_{\substack{\theta_s=\theta \\ \phi_s=\pi}}$$

or equivalently

$$\sigma^{\circ}_{Bj}(\theta) = \sigma^{\circ}_{Bj_0}(\theta) + \langle \sigma^{\circ}_{Bj_1}(\theta) \rangle \tag{3}$$

with

$$\sigma^{\circ}_{Bj_0}(\theta) = \cos\theta \cdot \gamma^{\circ}_j(\theta, \theta_s, \phi_s)\Big|_{\substack{\theta_s=\theta \\ \phi_s=\pi}} \tag{3a}$$

$$\langle \sigma^{\circ}_{Bj_1}(\theta) \rangle = \cos\theta \cdot \langle \gamma^{1}_j(\theta, \theta_s, \phi_s) \rangle\Big|_{\substack{\theta_s=\theta \\ \phi_s=\pi}} \tag{3b}$$

Detailed derivations of $\sigma^{\circ}_{Bj}(\theta)$ are given in section II.5.

II.2 Derivation of $\gamma^{\circ}_j(\theta, \theta_s, \phi_s)$

To derive $\gamma^{\circ}_j(\theta, \theta_s, \phi_s)$ we may begin with the vector scattered field due to a plane wave incident upon an undulating surface to which the tangent plane approximation is assumed applicable. Such a field expression is, in general, rather complicated. To simplify results, the stationary phase technique will be employed. An expression for $\gamma^{\circ}_j(\theta, \theta_s, \phi_s)$ not indicating explicitly the effect of the small irregularities will be derived first. This expression is then clarified to reflect the small structure effects by computing the explicit forms of the modified Fresnel reflection coefficients. As pointed out by Semyonov, such a computation may be performed for the more general finitely conducting surface in accordance with Rice's paper [13].

II.2.1 The scattered field

The far zone scattered field in the direction $\underline{n}_2$ due to a plane wave polarized along $\underline{a}$ impinging upon an undulating surface $Z(x,y)$ can be shown to be [14]

$$\underline{E}_{as} = K\,\underline{n}_2 \times \int \Big\{ \big[(1+\langle R_h \rangle)(\underline{a}\cdot\underline{t})(\underline{n}\times\underline{t}) - (1-\langle R_v \rangle)(\underline{a}\cdot\underline{d})(\underline{n}\cdot\underline{n}_1)\underline{t} \\ + \underline{n}_2 \times \big[(1+\langle R_v \rangle)(\underline{a}\cdot\underline{d})(\underline{n}\times\underline{t}) + (1-\langle R_h \rangle)(\underline{a}\cdot\underline{t})(\underline{n}\cdot\underline{n}_1)\underline{t} \big] \Big\} \\ \cdot E_o e^{-jk(\underline{n}_2-\underline{n}_1)\cdot\underline{r}}\, ds \tag{4}$$

where a time factor of the form $e^{j\omega t}$ has been suppressed; $K = \frac{-jke^{-jkR}}{4\pi R}$, R is the distance from the origin to the field point, k is the wave number; $\langle R_h \rangle, \langle R_v \rangle$ are the modified Fresnel reflection for horizontal and vertical polarization respectively; E_o is the magnitude of incident electric field; $\underset{\sim}{n}_1$ is the unit propagation vector of the incident field, and $\underset{\sim}{n}$ is the normal to the surface

The set of orthogonal unit vectors $(\underset{\sim}{n}_1, \underset{\sim}{t}, \underset{\sim}{d})$ serving as the local coordinates for evaluating the local field on surface is illustrated in Figure 2. The unit vectors, $\underset{\sim}{t}$ and $\underset{\sim}{d}$ relate to $\underset{\sim}{n}$ and $\underset{\sim}{n}_1$ as follows

$$\begin{aligned} \underset{\sim}{t} &= (\underset{\sim}{n}_1 \times \underset{\sim}{n}) / |\underset{\sim}{n}_1 \times \underset{\sim}{n}| \\ \underset{\sim}{d} &= \underset{\sim}{n}_1 \times \underset{\sim}{t} \end{aligned} \tag{5}$$

where $\underset{\sim}{n}$ may be written in terms of the partial derivatives, Z_x, Z_y of $Z(x, y)$ along x and y axes as follows

$$\underset{\sim}{n} = (-\underset{\sim}{i} Z_x - \underset{\sim}{j} Z_y + \underset{\sim}{k}) / (1 + Z_x^2 + Z_y^2)^{1/2},$$

$(\underset{\sim}{i}, \underset{\sim}{j}, \underset{\sim}{k})$ are the unit coordinate vectors.

To simplify (4) by the stationary phase approximation, let $\underset{\sim}{q} = \underset{\sim}{n}_2 - \underset{\sim}{n}_1$ and q_x, q_y, q_z be the vector components of $\underset{\sim}{q}$. Then the phase factor in (4) is

$$\underset{\sim}{q} \cdot \underset{\sim}{r} = q_x x + q_y y + q_z Z(x, y) \tag{6}$$

The stationary phase assumption requires

$$\frac{\partial}{\partial x}(\underset{\sim}{q} \cdot \underset{\sim}{r}) = \frac{\partial}{\partial y}(\underset{\sim}{q} \cdot \underset{\sim}{r}) = 0.$$

It follows that

$$\begin{aligned} Z_x &= -q_x / q_z \\ Z_y &= -q_y / q_z \\ \underset{\sim}{n} &= \underset{\sim}{q} / |\underset{\sim}{q}| \end{aligned} \tag{7}$$

The significant result indicated by (7) is that all surface slopes in (4) may be written in terms of the incident and scattered propagation vectors. Consequently, the integrand in (4) except for the phase factor, $\exp[-jk\,\underset{\sim}{q} \cdot \underset{\sim}{r}]$ can be moved outside of the integral sign, i.e.

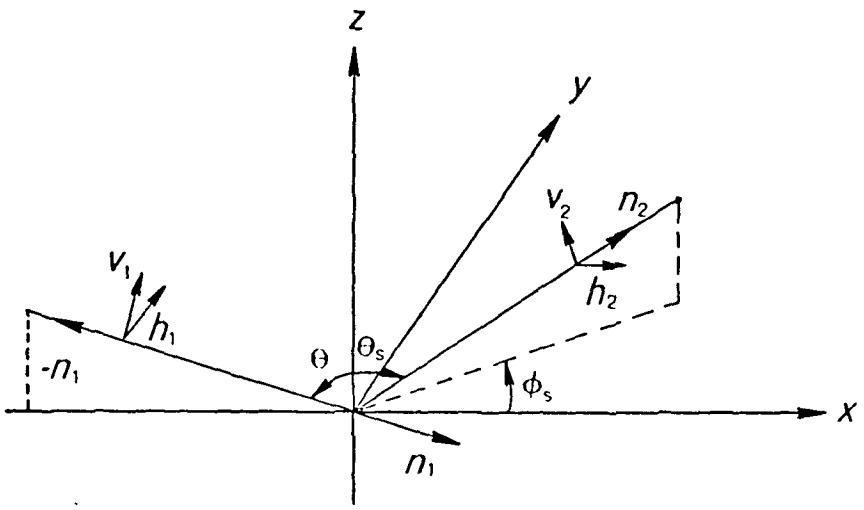

Figure 1.

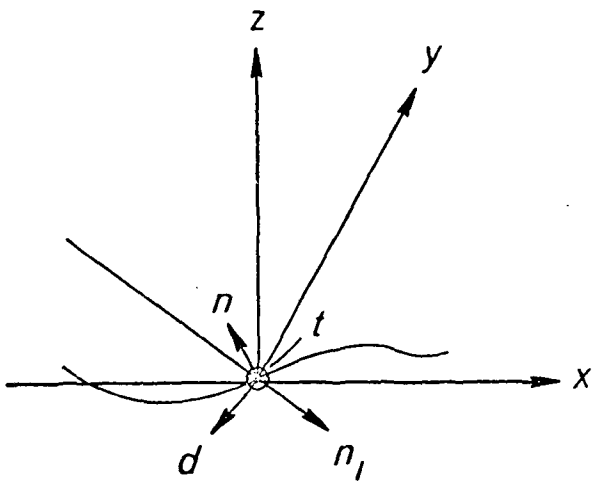

Figure 2.

$$\underset{\sim}{E}_{as} = E_o K \underset{\sim}{n}_2 \times \{(\underset{\sim}{A} - \underset{\sim}{B}) + \underset{\sim}{n}_2 \times (\underset{\sim}{C} + \underset{\sim}{D})\} \int_A e^{jk(\underset{\sim}{n}_2 - \underset{\sim}{n}_1)\cdot \underset{\sim}{r}} ds \tag{8}$$

with

$$\begin{aligned} \underset{\sim}{A} &= (1 + \langle R_h \rangle)(\underset{\sim}{a}\cdot\underset{\sim}{t})(\underset{\sim}{n}\times\underset{\sim}{t}) \\ \underset{\sim}{B} &= (1 - \langle R_v \rangle)(\underset{\sim}{a}\cdot\underset{\sim}{d})(\underset{\sim}{n}\cdot\underset{\sim}{n}_1)\,\underset{\sim}{t} \\ \underset{\sim}{C} &= (1 + \langle R_v \rangle)(\underset{\sim}{a}\cdot\underset{\sim}{d})(\underset{\sim}{n}\times\underset{\sim}{t}) \\ \underset{\sim}{D} &= (1 - \langle R_h \rangle)(\underset{\sim}{a}\cdot\underset{\sim}{t})(\underset{\sim}{n}\cdot\underset{\sim}{n}_1)\,\underset{\sim}{t} \end{aligned} \tag{9}$$

The local coordinate vectors, two other vector products in (9) and the differential surface element in (8) may all be written in terms of the propagation vectors,

$$\begin{aligned} \underset{\sim}{t} &= (\underset{\sim}{n}_1 \times \underset{\sim}{n}_2)/|\underset{\sim}{n}_1 \times \underset{\sim}{n}_2| \\ \underset{\sim}{d} &= \frac{(\underset{\sim}{n}_1\cdot\underset{\sim}{n}_2)\underset{\sim}{n}_1 - \underset{\sim}{n}_2}{|\underset{\sim}{n}_1 \times \underset{\sim}{n}_2|} \\ \underset{\sim}{n}\times\underset{\sim}{t} &= \frac{|\underset{\sim}{n}_2 - \underset{\sim}{n}_1|(\underset{\sim}{n}_1 + \underset{\sim}{n}_2)}{2|\underset{\sim}{n}_1 \times \underset{\sim}{n}_2|} \\ \underset{\sim}{n}\cdot\underset{\sim}{n}_1 &= \frac{-|\underset{\sim}{n}_2 - \underset{\sim}{n}_1|}{2} \\ ds &= (|\underset{\sim}{n}_2 - \underset{\sim}{n}_1|/q_z)\,dx\,dy \end{aligned} \tag{10}$$

To express the polarization states of both the incident and the scattered field, it is convenient to introduce a set of orthogonal unit vectors $(-\underset{\sim}{n}_1, \underset{\sim}{v}_1, \underset{\sim}{h}_1)$ for the incident field and another set $(\underset{\sim}{n}_2, \underset{\sim}{v}_2, \underset{\sim}{h}_2)$ for the scattered field (see Figure 1). In view of Figure 1, explicit expressions for these unit vectors may be written

$$\begin{aligned} -\underset{\sim}{n}_1 &= -\sin\theta\,\underset{\sim}{i} + \cos\theta\,\underset{\sim}{k} \\ \underset{\sim}{v}_1 &= \cos\theta\,\underset{\sim}{i} + \sin\theta\,\underset{\sim}{k} \\ \underset{\sim}{h}_1 &= \underset{\sim}{j} \end{aligned} \tag{11}$$

$$\begin{aligned} \underset{\sim}{n}_2 &= \sin\theta_s\cos\phi_s\,\underset{\sim}{i} + \sin\theta_s\sin\phi_s\,\underset{\sim}{j} + \cos\theta_s\,\underset{\sim}{k} \\ \underset{\sim}{v}_2 &= -\cos\theta_s\cos\phi_s\,\underset{\sim}{i} - \cos\theta_s\sin\phi_s\,\underset{\sim}{j} + \sin\theta_s\,\underset{\sim}{k} \\ \underset{\sim}{h}_2 &= \sin\phi_s\,\underset{\sim}{i} - \cos\phi_s\,\underset{\sim}{j} \end{aligned} \tag{12}$$

For horizontally polarized incident wave, $(\underset{\sim}{a} = \underset{\sim}{h}_1)$, the polarized and cross polarized scattered fields are given respectively by

$$\begin{aligned} E_{hh} &= \underset{\sim}{h}_2 \cdot \underset{\sim}{E}_{h,s} \\ &= E_o K \left[\underset{\sim}{h}_2 \cdot \underset{\sim}{n}_2 \times \{(\underset{\sim}{A}_h - \underset{\sim}{B}_h) + \underset{\sim}{n}_2 \times (\underset{\sim}{C}_h + \underset{\sim}{D}_h)\}\right] \int_A e^{-jk(\underset{\sim}{n}_2 - \underset{\sim}{n}_1)\cdot\underset{\sim}{r}} ds \\ E_{hv} &= \underset{\sim}{v}_2 \cdot \underset{\sim}{E}_{h,s} \\ &= E_o K \left[\underset{\sim}{v}_2 \cdot \underset{\sim}{n}_2 \times \{(\underset{\sim}{A}_h - \underset{\sim}{B}_h) + \underset{\sim}{n}_2 \times (\underset{\sim}{C}_h + \underset{\sim}{D}_h)\}\right] \int_A e^{-jk(\underset{\sim}{n}_2 - \underset{\sim}{n}_1)\cdot\underset{\sim}{r}} ds \end{aligned} \tag{13}$$

where

$$\underset{\sim}{A}_h = -|f|\,(1+\langle R_h\rangle)(\underset{\sim}{v}_1\cdot\underset{\sim}{n}_2)(\underset{\sim}{n}_1+\underset{\sim}{n}_2)$$

$$\underset{\sim}{B}_h = |f|\,(1-\langle R_v\rangle)(\underset{\sim}{h}_1\cdot\underset{\sim}{n}_2)(\underset{\sim}{n}_1\times\underset{\sim}{n}_2)$$

$$\underset{\sim}{C}_h = -|f|\,(1+\langle R_v\rangle)(\underset{\sim}{h}_1\cdot\underset{\sim}{n}_2)(\underset{\sim}{n}_1+\underset{\sim}{n}_2)$$

$$\underset{\sim}{D}_h = |f|\,(1-\langle R_h\rangle)(\underset{\sim}{v}_1\cdot\underset{\sim}{n}_2)(\underset{\sim}{n}_1\times\underset{\sim}{n}_2)$$

$$|f| = \frac{|\underset{\sim}{n}_2-\underset{\sim}{n}_1|}{2|\underset{\sim}{n}_1\times\underset{\sim}{n}_2|^2}$$

Similarly, for vertically polarized incident wave ($\underset{\sim}{a}=\underset{\sim}{v}_1$), the polarized and depolarized scattered fields are

$$\begin{aligned} E_{vh} &= \underset{\sim}{h}_2\cdot\underset{\sim}{E}_{v1s} \\ &= E_0 K\left[\underset{\sim}{h}_2\cdot\underset{\sim}{n}_2\times\left\{(\underset{\sim}{A}_v-\underset{\sim}{B}_v)+\underset{\sim}{n}_2\times(\underset{\sim}{C}_v+\underset{\sim}{D}_v)\right\}\right]\int_A e^{jk(\underset{\sim}{n}_2-\underset{\sim}{n}_1)\cdot\underset{\sim}{r}}\,ds \\ E_{vv} &= \underset{\sim}{v}_2\cdot\underset{\sim}{E}_{v1s} \\ &= E_0 K\left[\underset{\sim}{v}_2\cdot\underset{\sim}{n}_2\times\left\{(\underset{\sim}{A}_v-\underset{\sim}{B}_v)+\underset{\sim}{n}_2\times(\underset{\sim}{C}_v+\underset{\sim}{D}_v)\right\}\right]\int_A e^{jk(\underset{\sim}{n}_2-\underset{\sim}{n}_1)\cdot\underset{\sim}{r}}\,ds \end{aligned} \qquad (14)$$

where

$$\underset{\sim}{A}_v = |f|\,(1+\langle R_v\rangle)(\underset{\sim}{h}_1\cdot\underset{\sim}{n}_2)(\underset{\sim}{n}_1+\underset{\sim}{n}_2)$$

$$\underset{\sim}{B}_v = |f|\,(1-\langle R_v\rangle)(\underset{\sim}{v}_1\cdot\underset{\sim}{n}_2)(\underset{\sim}{n}_1\times\underset{\sim}{n}_2)$$

$$\underset{\sim}{C}_v = -|f|\,(1+\langle R_v\rangle)(\underset{\sim}{v}_1\cdot\underset{\sim}{n}_2)(\underset{\sim}{n}_1+\underset{\sim}{n}_2)$$

$$\underset{\sim}{D}_v = -|f|\,(1-\langle R_h\rangle)(\underset{\sim}{h}_1\cdot\underset{\sim}{n}_2)(\underset{\sim}{n}_1\times\underset{\sim}{n}_2)$$

The above field expressions may be further simplified using the vector identities

$$\underset{\sim}{h}_2\cdot\underset{\sim}{n}_2\times(\underset{\sim}{M}+\underset{\sim}{n}_2\times\underset{\sim}{N}) = \underset{\sim}{v}_2\cdot\underset{\sim}{M}-\underset{\sim}{h}_2\cdot\underset{\sim}{N}$$

$$\underset{\sim}{v}_2\cdot\underset{\sim}{n}_2\times(\underset{\sim}{M}+\underset{\sim}{n}_2\times\underset{\sim}{N}) = -\underset{\sim}{h}_2\cdot\underset{\sim}{M}-\underset{\sim}{v}_2\cdot\underset{\sim}{N}$$

Thus,

$$\begin{aligned} E_{hh} &= C_0(-\langle R_h\rangle bc + \langle R_v\rangle df)\,I \\ E_{hv} &= C_0(\langle R_h\rangle bf + \langle R_v\rangle dc)\,I \\ E_{vh} &= C_0(-\langle R_h\rangle df + \langle R_v\rangle bc)\,I \\ E_{vv} &= C_0(\langle R_h\rangle dc + \langle R_v\rangle bf)\,I \end{aligned} \qquad (15)$$

where $C_o = -jkE_o a_1 e^{-jkR} / (2\pi R \gamma_z |\underline{n}_2 \times \underline{n}_1|^2)$

$$I = \int_A e^{jk \underline{\gamma} \cdot \underline{r}} \, dx \, dy$$

$$\gamma_x = \sin\theta_s \cos\phi_s - \sin\theta$$

$$\gamma_y = \sin\theta_s \sin\phi_s$$

$$\gamma_z = \cos\theta + \cos\theta_s$$

$$b = (\underline{v}_1 \cdot \underline{n}_2) = \sin\theta\cos\theta_s + \cos\theta\sin\theta_s\cos\phi_s$$

$$c = (\underline{v}_2 \cdot \underline{n}_1) = -\sin\theta\cos\theta_s\cos\phi_s - \cos\theta\sin\theta_s$$

$$d = (\underline{h}_1 \cdot \underline{n}_2) = \sin\theta_s \sin\phi_s$$

$$f = (\underline{h}_2 \cdot \underline{n}_1) = \sin\theta \sin\phi_s$$

$$a_1 = |\underline{n}_2 - \underline{n}_1|^2 / 2 = 1 + \cos\theta\cos\theta_s - \sin\theta\sin\theta_s\cos\phi_s$$

$$|\underline{n}_2 \times \underline{n}_1|^2 = (c^2 + f^2) = (b^2 + d^2)$$

Note that by expressing $\underline{n}_2$ in terms of the orthogonal set $(\underline{n}_1, \underline{v}_1, \underline{h}_1)$ it can be shown that $|\underline{n}_2 \times \underline{n}_1|^2 = b^2 + d^2$. Similarly, by expressing $\underline{n}_1$ in terms of the orthogonal set $(\underline{n}_2, \underline{v}_2, \underline{h}_2)$, it also follows that $|\underline{n}_1 \times \underline{n}_2|^2 = c^2 + f^2$.

II.2.2 The differential scattering coefficients

The differential scattering coefficients related to the scattered fields computed in the previous section [12, 15] are of the form

$$\gamma_{j,i}(\theta, \theta_s, \phi_s) = \frac{4\pi R^2 \langle E_{ji} E_{ji}^* \rangle}{E_o^2 A_o \cos\theta} \tag{16}$$

where the symbol * denotes complex conjugate, and $\langle \cdots \rangle$ the ensemble average. The subscripts j, i denote the polarization states of the incident and the scattered fields respectively. A_o is the illuminated area.

Upon substituting (15) into (16), it follows that

$$\begin{aligned}
\gamma_h^o(\theta, \theta_s, \phi_s) &= \gamma_{hh}^o(\theta, \theta_s, \phi_s) + \gamma_{hv}^o(\theta, \theta_s, \phi_s) \\
&= \frac{k^2 a_1^2}{\pi A_o \cos\theta \, \gamma_z^2} \left[\frac{|\langle R_h \rangle|^2 b^2 + |\langle R_v \rangle|^2 d^2}{b^2 + d^2} \right] \langle |I|^2 \rangle \\
\gamma_v^o(\theta, \theta_s, \phi_s) &= \gamma_{vh}^o(\theta, \theta_s, \phi_s) + \gamma_{vv}^o(\theta, \theta_s, \phi_s) \\
&= \frac{k^2 a_1^2}{\pi A_o \cos\theta \, \gamma_z^2} \left[\frac{|\langle R_v \rangle|^2 b^2 + |\langle R_h \rangle|^2 d^2}{b^2 + d^2} \right] \langle |I|^2 \rangle
\end{aligned} \tag{17}$$

For an isotropically rough surface with Gaussian height distribution, $\langle |I|^2 \rangle$ simplifies to

$$\langle |I|^2 \rangle = 2\pi A_o \int J_o(k\sqrt{q_x^2+q_y^2}\,\xi)\, e^{-k^2 q_z^2 \sigma^2 [1-\rho(\xi)]}\, \xi\, d\xi \qquad (18)$$

where $J_o(\ )$ is the zero order Bessel function of the first kind; σ^2 and $\rho(\xi)$ are the variance and the autocorrelation coefficient of the surface respectively.

An approximate solution for (18) consistent with the stationary phase approximation is

$$\langle |I|^2 \rangle = \frac{2\pi A_o}{k^2 q_z^2 m^2} \exp\left[-\frac{q_x^2+q_y^2}{2 q_z^2 m^2}\right] \qquad (19)$$

where $m = [\sigma^2 |\rho''(0)|]^{\frac{1}{2}}$ is the rms slope of the surface.

II.3 Derivation of $\langle \gamma_j^1(\theta, \theta_s, \phi_s) \rangle$

The scattered field due only to the small irregularities has been derived by many investigators [13,16,17]. As indicated in the previous section, with the scattered field expression known the scattering coefficient can be computed. To account for the interaction between the small irregularities and the large undulations, the expression for the scattering coefficient of the small irregularities is then averaged with respect to the slope distribution of the large undulations. The resulting expression is the desired scattering coefficient, $\langle \gamma_j^1(\theta, \theta_s, \phi_s) \rangle$.

II.3.1 Differential scattering coefficients

The far zone scattered field of i-polarization along the direction defined by the angles θ_s' and ϕ_s' due to a plane wave of j-polarization with unit amplitude impinging upon an irregular surface $s(x,y)$ along the direction defined by the angles θ' and ϕ' has been derived by using the method of small perturbation [17]. The ensemble average of the magnitude square of the scattered field, $\langle |E_{ji}(\theta', \phi', \theta_s', \phi_s')|^2 \rangle$ can be shown to be [17]

$$\langle |E_{ji}(\theta', \phi', \theta_s', \phi_s')|^2 \rangle = \frac{k^4 A_o}{R^2} \cos^2\theta' \cos^2\theta_s' |M_{ji}|^2 W(p,q) \qquad (20)$$

where

$j.i.$ = incident and scattered polarizations respectively, either horizontal or vertical polarizations,

A_o = illuminated area,

R = distance from the field point to the surface,

$$M_{hh} = \frac{(\epsilon_r - 1)\cos(\phi_s' - \phi')}{(\cos\theta' + \sqrt{\epsilon_r - \sin^2\theta'})(\cos\theta_s' + \sqrt{\epsilon_r - \sin^2\theta_s'})}$$

$$M_{hv} = \frac{(\epsilon_r - 1)\sin(\phi_s' - \phi')\sqrt{\epsilon_r - \sin^2\theta_s'}}{(\cos\theta' + \sqrt{\epsilon_r - \sin^2\theta'})(\epsilon_r\cos\theta_s' + \sqrt{\epsilon_r - \sin^2\theta_s'})} \qquad (21)$$

$$M_{vh} = \frac{-(\epsilon_r - 1)\sin(\phi_s' - \phi')\sqrt{\epsilon_r - \sin^2\theta'}}{(\epsilon_r\cos\theta' + \sqrt{\epsilon_r - \sin^2\theta'})(\cos\theta_s' + \sqrt{\epsilon_r - \sin^2\theta_s'})}$$

$$M_{vv} = \frac{-(\epsilon_r - 1)\left[\cos(\phi_s' - \phi')\sqrt{\epsilon_r - \sin^2\theta'}\sqrt{\epsilon_r - \sin^2\theta_s'} - \epsilon_r \sin\theta_s' \sin\theta'\right]}{(\epsilon_r\cos\theta' + \sqrt{\epsilon_r - \sin^2\theta'})(\epsilon_r\cos\theta_s' + \sqrt{\epsilon_r - \sin^2\theta_s'})}$$

ϵ_r = complex relative dielectric constant,

$W(p,q)$ = surface roughness spectral density,

$$p = k\left[\sin\theta_s' \cos(\phi_s' - \phi') - \sin\theta'\right]$$

$$q = k \sin\theta_s' \sin(\phi_s' - \phi')$$

Note that the surface roughness spectral density $W(p,q)$, is related to its correlation function $R(x,y)$ by

$$R(x,y) = \frac{1}{4}\int_{-\infty}^{\infty}\int_{-\infty}^{\infty} W(p,q)\, e^{jpx + jqy}\, dp\, dq$$

For an isotropically rough surface, it reduces to

$$R(r) = \frac{\pi}{2}\int_0^{\infty} W(t)\, J_0(tr)\, t\, dt$$

and

$$W(t) = \frac{2}{\pi}\int_0^{\infty} R(r)\, J_0(tr)\, r\, dr$$

For a Gaussian spectral density, it is expressed in the form

$$W(t) = \frac{\sigma_1^2 \ell^2}{\pi} \exp\left[-\left(\frac{\ell t}{2}\right)^2\right] \qquad (22)$$

where

$$t = \sqrt{p^2 + q^2}$$

σ_1, ℓ = standard deviation and correlation length of the small irregularities respectively.

From (16) and the relation

$$\gamma_j^1(\theta',\phi',\theta_s',\phi_s') = \gamma_{jh}^1(\theta',\phi',\theta_s',\phi_s') + \gamma_{jv}^1(\theta',\phi',\theta_s',\phi_s')$$

we get

$$\gamma_j^1(\theta',\phi',\theta_s',\phi_s') = 4k^4\sigma_1^2\ell^2\cos\theta'\cos^2\theta_s'\left[|M_{jh}|^2+|M_{jv}|^2\right]\exp\left[-\left(\frac{\ell t}{2}\right)^2\right] \tag{23}$$

$$j = h \text{ or } v$$

II.3.2 Averaging Procedure

To account for the tilting effect of the small irregularities by the large undulations it is necessary to average $\gamma_j^1(\theta',\phi',\theta_s',\phi_s')$ with respect to the slope distribution of the large undulations [8]. That is

$$\langle \gamma_j^1(\theta,\theta_s,\phi_s)\rangle = \int_{-\infty}^{\infty}\int_{-\infty}^{\infty}\gamma_j^1(\theta',\phi',\theta_s',\phi_s')\,p(z_x,z_y)\sqrt{1+z_x^2+z_y^2}\;dz_x\,dz_y \tag{24}$$

where θ is the incident angle and θ_s and ϕ_s are the scattering angles.

To evaluate the above integral, connecting relations between the surface slopes z_x, z_y and the local angles, $\theta', \phi', \theta_s', \phi_s'$ are needed. To find these relations let us first express z_x and z_y in terms of the azimuth and the elevation angles, ϕ_n and θ_n, which represent the tilting effect

$$z_x = \cos\phi_n \tan\theta_n \tag{25}$$

$$z_y = \sin\phi_n \tan\theta_n$$

From (25) it follows that

$$\sqrt{1+z_x^2+z_y^2} = \sec\theta_n$$

$$dz_x\,dz_y = \left|\frac{\partial(z_x,z_y)}{\partial(\theta_n,\phi_n)}\right| d\theta_n d\phi_n = \sec^3\theta_n \sin\theta_n\, d\theta_n\, d\phi_n \tag{26}$$

The local angles $(\theta', \phi', \theta_s', \phi_s')$ may now be related to the azimuth and the elevation angles ϕ_n and θ_n by connecting relations derived below.

In Figure 3, the two sets of coordinates (x,y,z) and (x', y', z') are related in terms of the angles θ_n and ϕ_n as follows:

$$\begin{bmatrix} x' \\ y' \\ z' \end{bmatrix} = \begin{bmatrix} \cos\theta_n \cos\phi_n & \cos\theta_n \sin\phi_n & \sin\theta_n \\ -\sin\phi_n & \cos\phi_n & 0 \\ -\sin\theta_n \cos\phi_n & -\sin\theta_n \sin\phi_n & \cos\theta_n \end{bmatrix} \begin{bmatrix} x \\ y \\ z \end{bmatrix} \tag{27}$$

Hence, for a scattered field point, P, located at a distance, R, from the origin, the coordinates of P may be expressed either in terms of the angles θ_s' and ϕ_s' or the angles θ_s and ϕ_s ,

$$\begin{aligned} x' &= R \sin\theta_s' \cos\phi_s' \\ y' &= R \sin\theta_s' \sin\phi_s' \\ z' &= R \cos\theta_s' \end{aligned} \tag{28a}$$

$$\begin{aligned} x &= R \sin\theta_s \cos\phi_s \\ y &= R \sin\theta_s \sin\phi_s \\ z &= R \cos\theta_s \end{aligned} \tag{28b}$$

Substituting equation (28) into (27) we obtain the connecting equations for the sets of angles as follows:

$$\begin{bmatrix} \sin\theta_s' \cos\phi_s' \\ \sin\theta_s' \sin\phi_s' \\ \cos\theta_s' \end{bmatrix} = \begin{bmatrix} \cos\theta_n \cos\phi_n & \cos\theta_n \sin\phi_n & \sin\theta_n \\ -\sin\phi_n & \cos\phi_n & 0 \\ -\sin\theta_n \cos\phi_n & -\sin\theta_n \sin\phi_n & \cos\theta_n \end{bmatrix} \begin{bmatrix} \sin\theta_s \cos\phi_s \\ \sin\theta_s \sin\phi_s \\ \cos\theta_s \end{bmatrix} \tag{29}$$

If we take the angles with a prime to be local scattering angles, we see from (29) that the local scattering angles may be expressed in terms of the scattering angles θ_s, ϕ_s and the tilting angles θ_n , ϕ_n , i.e.

$$\begin{aligned} \cos\theta_s' &= \cos\theta_n \cos\theta_s - \sin\theta_n \sin\theta_s \cos(\phi_s - \phi_n) \\ \sin\phi_s' &= \sin\theta_s \sin(\phi_s - \phi_n)(1 - \cos^2\theta_s')^{-\frac{1}{2}} \end{aligned} \tag{30}$$

In a similar fashion, the local incident angles can also be expressed in terms of the tilting angles θ_n, ϕ_n and the incident angle, θ .

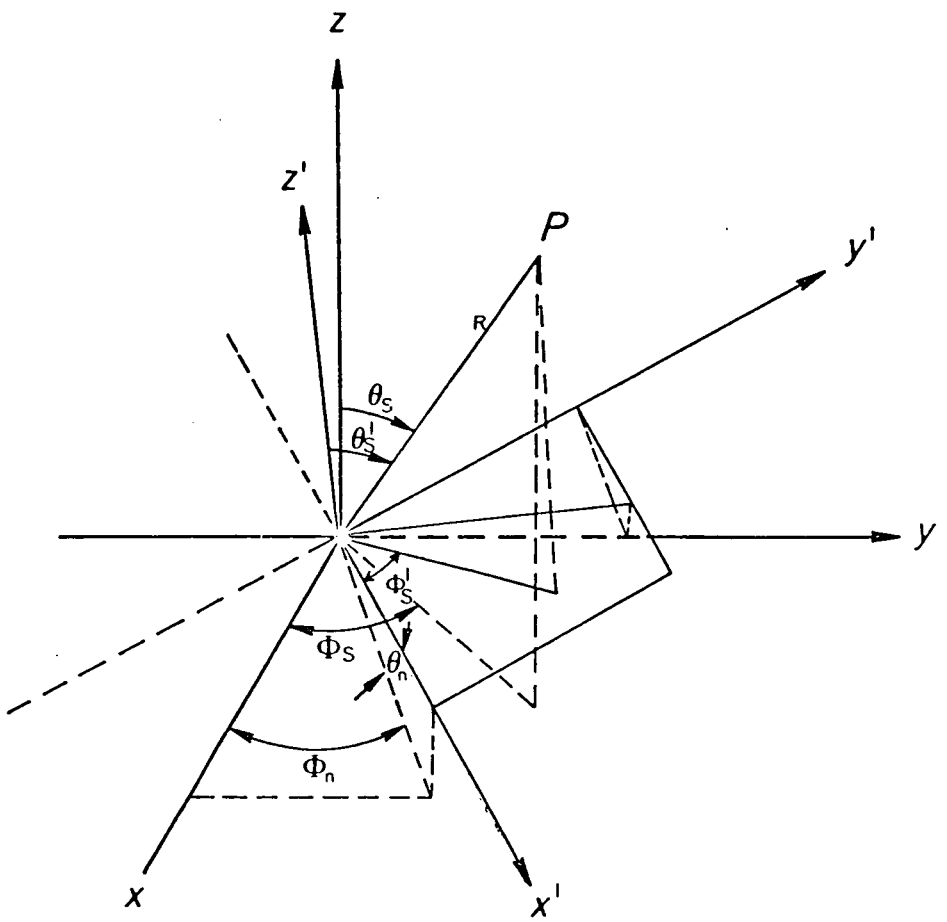

Figure 3.

$$\cos\theta' = \cos\theta_n \cos\theta + \sin\theta_n \sin\theta \cos\phi_n$$

$$\sin\phi' = -\sin\theta \sin\phi_n \left(1-\cos^2\theta\right)^{-1/2} \tag{31}$$

With the connecting relations between the local angles and the surface slopes known (24) can be evaluated by assuming a form for P(Zx,Zy). For a Gaussian surface slope distribution it may be represented as

$$P(Z_x, Z_y) = \frac{1}{2\pi m^2} \; e^{-\frac{Z_x^2 + Z_y^2}{2m^2}} \tag{32}$$

or equivalently

$$P(\theta_n, \phi_n) = \frac{1}{2\pi m^2} \; e^{-\frac{\tan^2\theta_n}{2m^2}} \tag{33}$$

where m is the rms slope and is assigned according to Cox and Munk's slick sea data.

Since m^2 is usually sufficiently small for the sea and since $\gamma_j^1(\theta', \phi', \theta_s', \phi_s')$ is insensitive to θ_n for a small value of θ_n, the integration with respect to θ_n given in (24) can be evaluated by the method of steepest decent; if so, the result may be expressed as

$$\langle \gamma_j^1(\theta, \theta_s, \phi_s) \rangle = \frac{1}{2\pi} \int_{-\frac{\pi}{2}}^{\frac{\pi}{2}} \left\{ \gamma_j^1(\theta', \phi', \theta_s', \phi_s') \Big|_{\theta_n = \tan^{-1}(m)} + \gamma_j^1(\theta', \phi', \theta_s', \phi_s') \Big|_{\theta_n = -\tan^{-1}(m)} \right\} d\phi_n \tag{34}$$

II.4 Modified Fresnel Reflection Coefficients

As mentioned in section II.2, the Fresnel reflection coefficients should be modified to account for the presence of the small irregularities [12] [8]. The method for computing these coefficients has been discussed by Rice for horizontally polarized waves. Following Rice's approach also for the vertically polarized wave, we obtain the modified Fresnel reflection coefficients as follows

$$\langle R_h \rangle = R_h(\Theta) \left\{ 1 - 2k^2 \cos\Theta \int_{-\infty}^{+\infty} \int_{-\infty}^{+\infty} \frac{W(u - k\sin\Theta, v)}{4} \left[\sqrt{\epsilon_r - \sin^2\Theta} - \frac{(c-b)(u^2+bc)}{k(u^2+v^2+bc)} \right] du\, dv \right\} \tag{35a}$$

$$\langle R_v \rangle = R_v(\Theta) \left\{ 1 - \frac{2k^2\cos\Theta}{(\cos^2\Theta - \frac{\sin^2\Theta}{\epsilon_r})} \int_{-\infty}^{\infty} \int_{-\infty}^{\infty} \frac{W(u - k\sin\Theta, v)}{4} \left[\sqrt{\epsilon_r - \sin^2\Theta} - \frac{1}{(u^2+v^2+bc)} \right. \right.$$

$$\left. \left. \left\{ \frac{(c-b)}{k} \left[v^2 + bc - \frac{\sin^2\Theta}{\epsilon_r} - (u^2+v^2)\sin^2\Theta \right] + 2k^2 \sqrt{\epsilon_r - \sin^2\Theta}\; u \right\} \right] du\, dv \right\} \tag{35b}$$

where

$$R_h(\Theta) = \frac{\cos\Theta - \sqrt{\epsilon_r - \sin^2\Theta}}{\cos\Theta + \sqrt{\epsilon_r - \sin^2\Theta}}$$

$$R_v(\Theta) = \frac{\epsilon_r\cos\Theta - \sqrt{\epsilon_r - \sin^2\Theta}}{\epsilon_r\cos\Theta + \sqrt{\epsilon_r - \sin^2\Theta}} \qquad (36)$$

$$\cos\Theta = \frac{1}{\sqrt{2}}\left(1 + \cos\theta\cos\theta_s - \sin\theta\sin\theta_s\cos\phi_s\right)^{\frac{1}{2}}$$

ϵ_r = complex relative dielectric constant

$$c = \sqrt{k^2\epsilon_r - (u^2+v^2)}$$

$$b = \sqrt{k^2 - (u^2+v^2)}$$

For the special case where

$$W(u - k\sin\Theta, v) = \frac{\ell^2\sigma_1^2}{\pi}\exp\left[-\frac{\ell^2}{4}(u^2+v^2-2ku\sin\Theta + k^2\sin^2\Theta)\right] \qquad (37)$$

$|\langle R_j\rangle|^2$ simplifies to

$$|\langle R_j\rangle|^2 = |R_j|^2\left\{1 - 4k^2\sigma_1^2\cos\Theta\exp\left(-\tfrac{1}{2}\sin^2\Theta\right)\right\} \qquad j = h \text{ or } v \qquad (38)$$

II.5 Backscattering cross-sections

Substituting $\theta_s = \theta$ and $\phi_s = \pi$ into (36) we obtain

$$R_h(0) = -R_v(0) = \frac{1-\sqrt{\epsilon_r}}{1+\sqrt{\epsilon_r}}$$

and

$$|\langle R_h(0)\rangle|^2 = |\langle R_v(0)\rangle|^2 = \left|\frac{1-\sqrt{\epsilon_r}}{1+\sqrt{\epsilon_r}}\right|^2(1 - 4.0\,k^2\sigma_1^2) \qquad (39)$$

From (17), (19) and (3a), it follows that

$$\sigma^o_{Bho}(\theta) = \sigma^o_{Bvo}(\theta) = \frac{|\langle R_h(0)\rangle|^2}{2m^2\cos^4\theta}\, e^{-\frac{\tan^2\theta}{2m^2}} \qquad (40)$$

Equation (40) shows that the backscattering cross-section of the large undulations is polarization independent.

To find $\langle \sigma^{\circ}_{Bj1} \rangle$, note the following two points:

(1) Substituting $\theta_s = \theta$ and $\phi_s = \pi$ into (30) we obtain

$$\cos\theta_s' = \cos\theta' = \cos\theta_n \cos\theta + \sin\theta_n \cos\phi_n \sin\theta$$
$$\sin\phi_s' = -\sin\phi' = \sin(\phi' + \pi) \tag{41}$$

or

$$\theta_s' = \theta'$$
$$\phi_s' = \phi' + \pi$$

(2) Since $\theta_s = \theta$ and $\phi_s = \pi$ imply $\theta_s' = \theta'$ and $\phi_s' = \phi' + \pi$, from (34) it follows that

$$\langle \gamma_j^1(\theta, \theta_s, \phi_s) \rangle \Big|_{\substack{\theta_s = \theta \\ \phi_s = \pi}} = \frac{1}{2\pi} \int_{-\frac{\pi}{2}}^{\frac{\pi}{2}} \left\{ \gamma_j^1(\theta', \phi', \theta_s', \phi_s') \Big|_{\substack{\theta_n = \tan^{-1}(m) \\ \theta_s' = \theta' \\ \phi_s' = \phi' + \pi}} + \gamma_j^1(\theta', \phi', \theta_s', \phi_s') \Big|_{\substack{\theta_n = -\tan^{-1}(m) \\ \theta_s' = \theta' \\ \phi_s' = \phi' + \pi}} \right\} d\phi_n \tag{42}$$

Thus from (3b) and (42),

$$\langle \sigma^{\circ}_{Bj1}(\theta) \rangle = \frac{1}{2\pi} \int_{-\frac{\pi}{2}}^{\frac{\pi}{2}} \left\{ \sigma^{\circ}_{Bj1}(\theta') \Big|_{\theta_n = \tan^{-1}(m)} + \sigma^{\circ}_{Bj1}(\theta') \Big|_{\theta_n = -\tan^{-1}(m)} \right\} d\phi_n \tag{43}$$

$$j = h \text{ or } v$$

where

$$\sigma^{\circ}_{Bh1}(\theta') = \cos\theta' \cdot \gamma_h^1(\theta', \phi', \theta_s', \phi_s') \Big|_{\substack{\phi_s' = \phi' + \pi \\ \theta_s' = \theta'}}$$
$$= 4k^4 \sigma_1^2 \ell^2 \cos^4\theta' \left| R_h(\theta') \right|^2 e^{-k^2\ell^2 \sin^2\theta'} \tag{44}$$

$$\sigma^{\circ}_{Bv1}(\theta') = \cos\theta' \cdot \gamma_v^1(\theta', \phi', \theta_s', \phi_s') \Big|_{\substack{\phi_s' = \phi + \pi \\ \theta_s' = \theta'}}$$
$$= 4k^4 \sigma_1^2 \ell^2 \cos^4\theta' \left| \frac{(\epsilon_r - 1)\left[(\epsilon_r - 1)\sin^2\theta' + \epsilon_r\right]}{\left(\epsilon_r \cos\theta' + \sqrt{\epsilon_r - \sin^2\theta'}\right)^2} \right|^2 e^{-k^2\ell^2 \sin^2\theta'} \tag{45}$$

The complete backscattering cross-section is, of course, given by (3) that is the sum of (40) and (43).

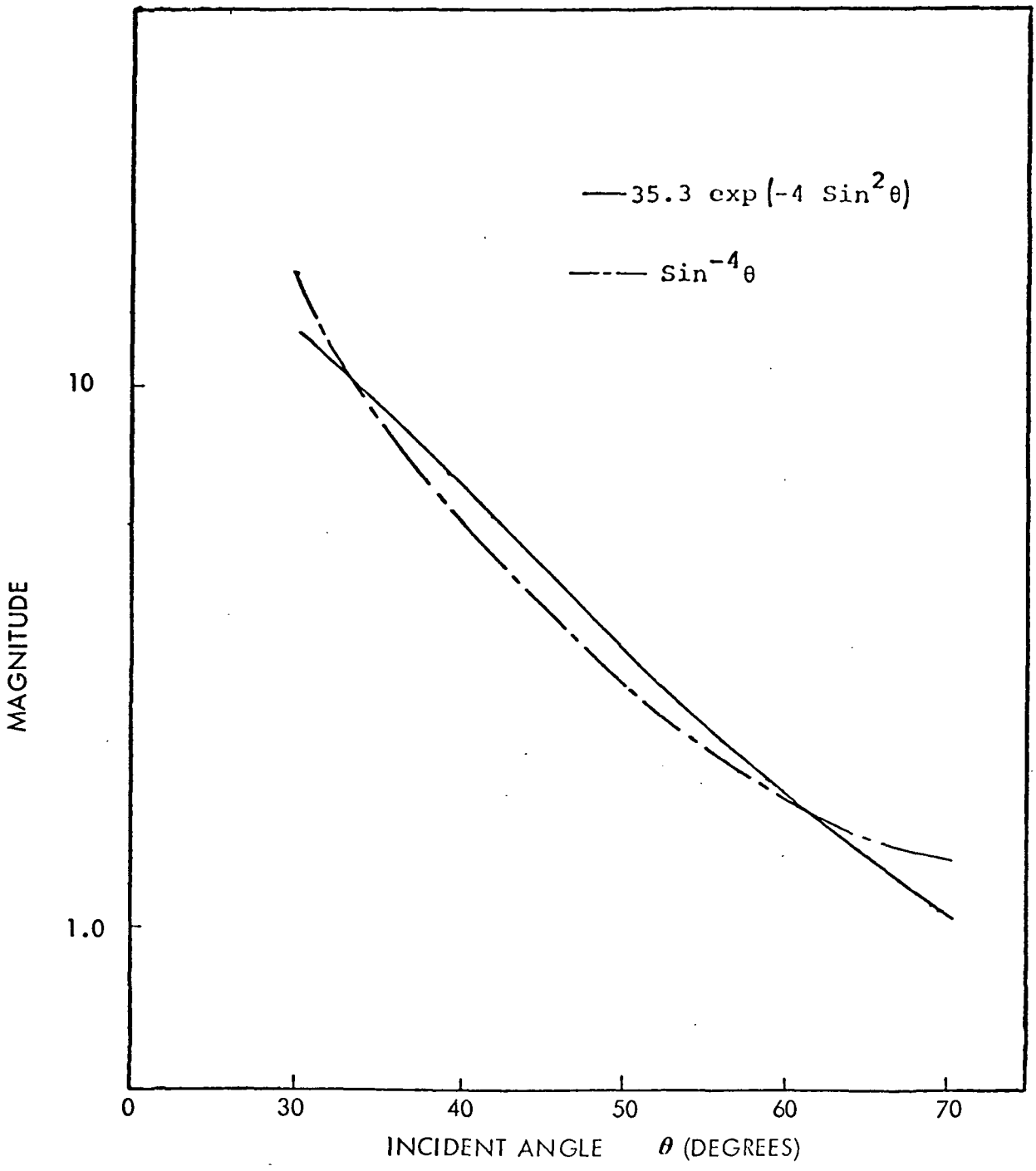

Figure 4. Comparison of the angular variation of $\sin^{-4}\theta$ and $35.3\ exp\,(-4\sin^2\theta)$

III. SELECTION OF PARAMETERS

The surface parameters appear in the above theory are the rms slope of the large structures m, the standard deviation of the small structures σ_1, and the correlation length of the small structures ℓ. This scattering model can be adapted to predict sea returns by noting that the rms slope can be based on measurements by Cox and Munk [7] and that the assumed Gaussian spectrum for the small irregularities can approximate the high frequency portion of the sea spectrum BK^{-4} where the Bragg scatter condition applies, i.e., $K = 2k \sin \Theta$. In view of the requirements of the composite surface theory it is reasonable to choose the oil slick sea measurements by Cox and Munk, since the small irregularities have been suppressed. The value of m is thus assigned. The value of $k\ell$ is assigned so that the correct angular behavior of the Gaussian spectrum approximated BK^{-4} well over the angular range, $30^\circ \leq \Theta \leq 70^\circ$, i.e., BK^{-4} is approximated by $\sigma_1^2 \ell^2/\pi \exp(-K^2\ell^2/4)$ where $K = 2k \sin \Theta$, the Bragg scatter condition. This is achieved by noting that when $k\ell = 2$ similar behavior is realized (see Figure 4). The factor 35.3 appears in the Gaussian approximation to bring the levels into agreement at $\Theta = 60$ degrees. The value of B must yet be assigned.

Oceanographic investigations indicate values of B in the range from 4.6×10^{-3} to 3.26×10^{-2} [7,18,19]. This implies that $k\sigma_1$ should lie in the range from 0.084 to 0.24 when BK^{-4} is equated to $\sigma_1^2 \ell^2/\pi \exp(-K^2\ell^2/4)$ at $\Theta = 60$ degrees. These values of $k\sigma_1$ are consistent with the assumptions of the small perturbation theory, an encouraging result. The recent reports by Sutherland [11] and Pierson [20] indicate that B is a function of the wind speed. Thus, the surface parameter σ_1 must also be a function of the wind speed. It is noted that the horizontally polarized emission characteristic for nadir angles from zero to thirty degrees is very sensitive to $k\sigma_1$ and hence the parameter $k\sigma_1$ can be estimated by fitting the predicted emission characteristics to the measured data.*

With the surface parameters established in the manner described above, both the emission and the backscatter characteristics may be computed and compared with reported measurements.

*It appears that the wind sensitivity of B may be assigned by this technique.

IV. COMPARISON WITH EXPERIMENTS

The parameter $k\sigma_1$ is estimated from horizontally polarized emission characteristics at 8.36 GHz associated with two distinct wind speeds. The emission characteristics are based on an average of several of Hollinger's experiment runs* under similar wind stress conditions.** The vertically polarized emission characteristic is then computed from the estimated $k\sigma_1$. These results are shown in the graphs of Figures 5 and 6. The dielectric constant is based on data reported by Saxton and Lane [10].

Comparison of the predictions of this emission model indicates a significantly improved agreement over that predicted by a single surface model. Better level and trend agreement is evident for both horizontally and vertically polarized emissions. Sensitivity to wind speed is evident at nadir which is not noted with the single surface model. The sensitivity at nadir is carried by the modified Fresnel coefficient (see Equation (38)).

The adequacy of the composite surface theory is further demonstrated when the predicted backscatter characteristics are compared with measured characteristics. Data at 8.91 GHz reported by Daley, et al., *** [22] at similar wind stress conditions were chosen as a basis for comparison. The dielectric constant is changed to reflect the influence of the slightly different frequency. The comparison of predicted and measured characteristics are shown in Figure 7 through 10. These results indicate reasonable agreement with measurements and improved agreement over the predictions of the simple geometric optics approach (single surface model). It is noted that the best agreement with measurements occurs primarily at larger angles and for vertical polarization. There is some uncertainty in the accuracy of the measurements near nadir [22] so lack of agreement may be anticipated there. The discrepancy at large angles for horizontally polarized cross sections may be attributable to receiver noise at these small cross sections. This statement is, however, speculative.

*The authors are indebted to Dr. J. P. Hollinger of NRL for making his radiometric measurements available to us. His data with foam and atmospheric effects removed are appropriate to compare with the authors calculations.

**The authors are also grateful to Dr. V. J. Cardone of NYU for interpreting Hollinger's wind speed measurements under comparable wind stress conditions.

***The authors are indebted to Mr. N. W. Guinard of NRL for making these backscatter data available to us.

The level of NRL data which are based on the statistical median had to be raised by 6 dB to realize the agreement. Valenzuela [23] indicated that the average cross section was about 4.6 dB above the median based on exponential statistics assumed for the returns. As a consequence, 1.4 dB remains unaccounted for. Perhaps the remaining 1.4 dB may be partially associated with the biases disclosed by Claassen and Fung. [24]

V. CONCLUSIONS

A bistatic two scale non-coherent scattering theory extended from Symyonov's paper [8] has been developed to yield the expressions for the differential scattering coefficients. The emission and the backscattering characteristics are then derived from the differential scattering coefficients in the standard way. The theory assumed Gaussian surface height distributions and Gaussian correlation functions for both scales of roughness.

The emission and the scattering characteristics are shown to be dependent on the rms slope of the large undulations m, the standard deviation of the small irregularities σ_1 , and the correlation length of the small irregularities ℓ . The wind dependence of the first two parameters is associated with m through slick sea measurements by Cox and Munk, and the σ_1 through the high frequency sea spectrum. The parameter ℓ is associated with the shape of the high frequency sea spectrum and can be reasonably chosen by fitting the sea spectrum BK^{-4} to the assumed Gaussian spectrum.

It is noted that the emission characteristic for horizontal polarization is a sensitive measure of σ_1. Thus, σ_1 is established by fitting the emission characteristic to measured data for different wind speeds. The parameters chosen in this way are then used to compute the vertically polarized emission characteristic. Good agreement with measured data and better agreement than a simple surface model are demonstrated.

The same set of surface parameters at each wind speed is then used to compute the backscatter characteristics. The results except for level are shown to agree reasonably over all angles with NRL backscatter data under similar wind conditions. Comparison of these characteristics with a single parameter surface model demonstrated better results.

These findings have proven that the validity of scattering theories is better demonstrated when both the predicted backscatter and the emission characteristics are compared with measurements. They have further shown that the measured emission and scattering characteristics with the aid of a reasonable composite surface theory may aid the oceanographer in identifying the wind dependence of the sea spectrum.

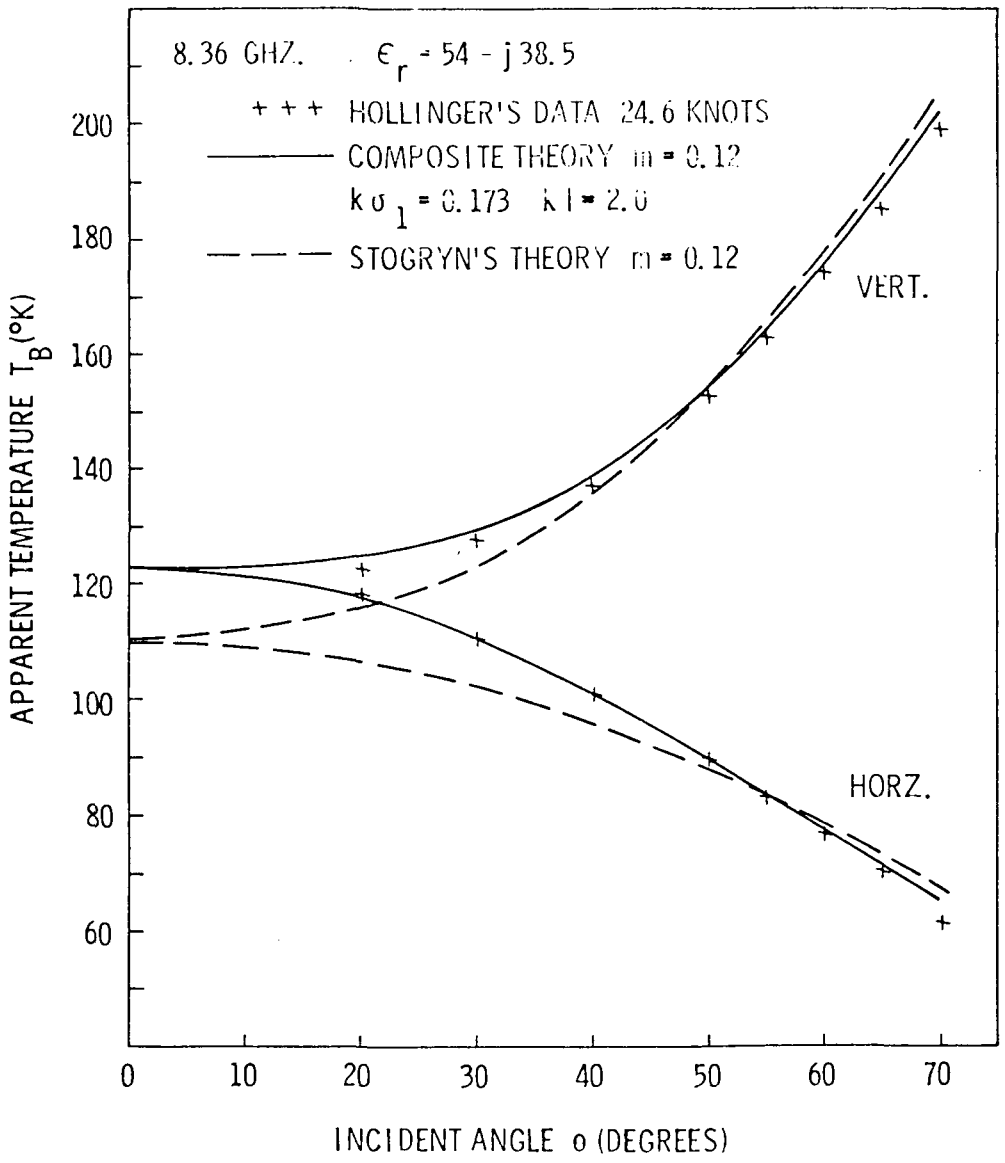

Figure 5. Comparison of computed and measured emission characteristics.

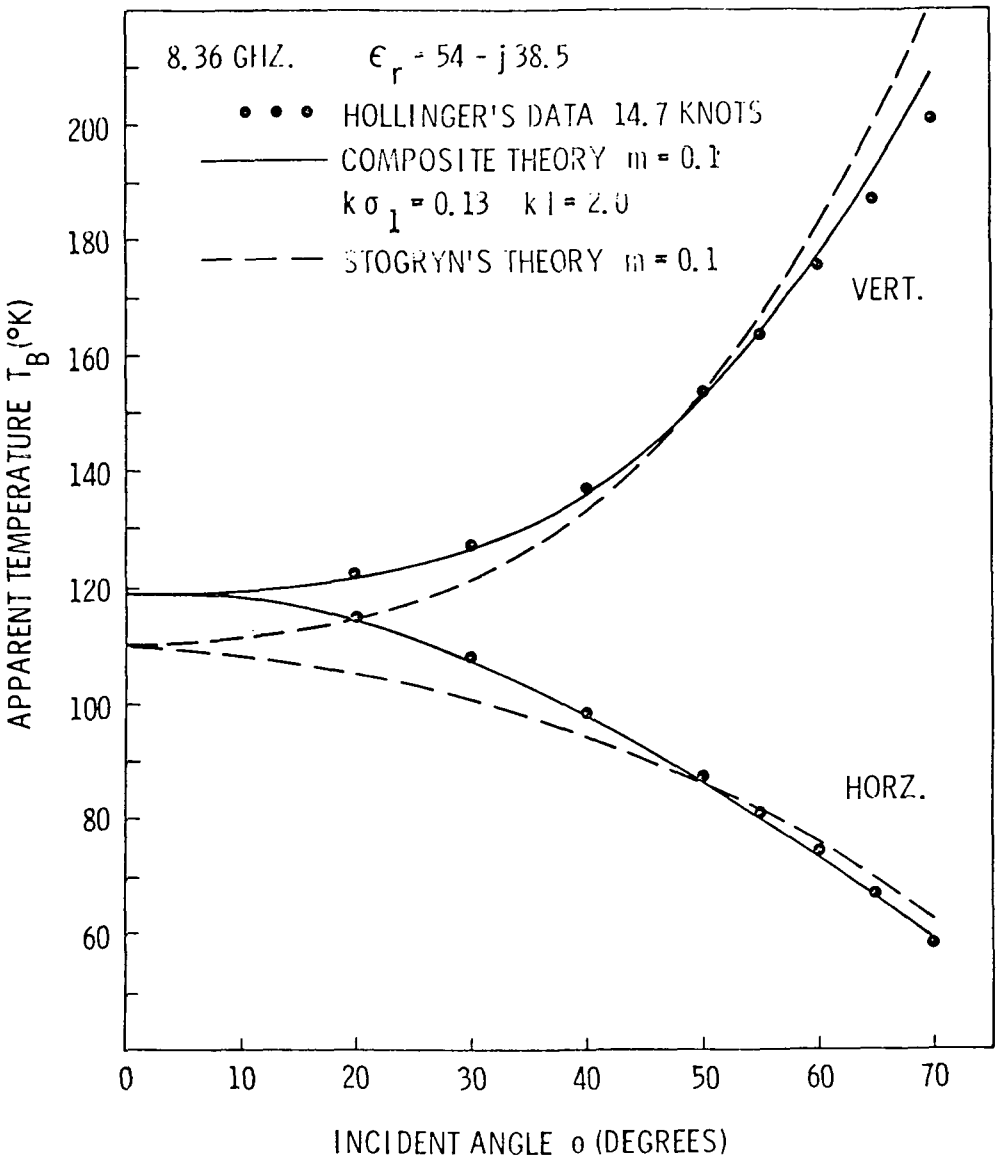

Figure 6. Comparison of computed and measured emission characteristics.

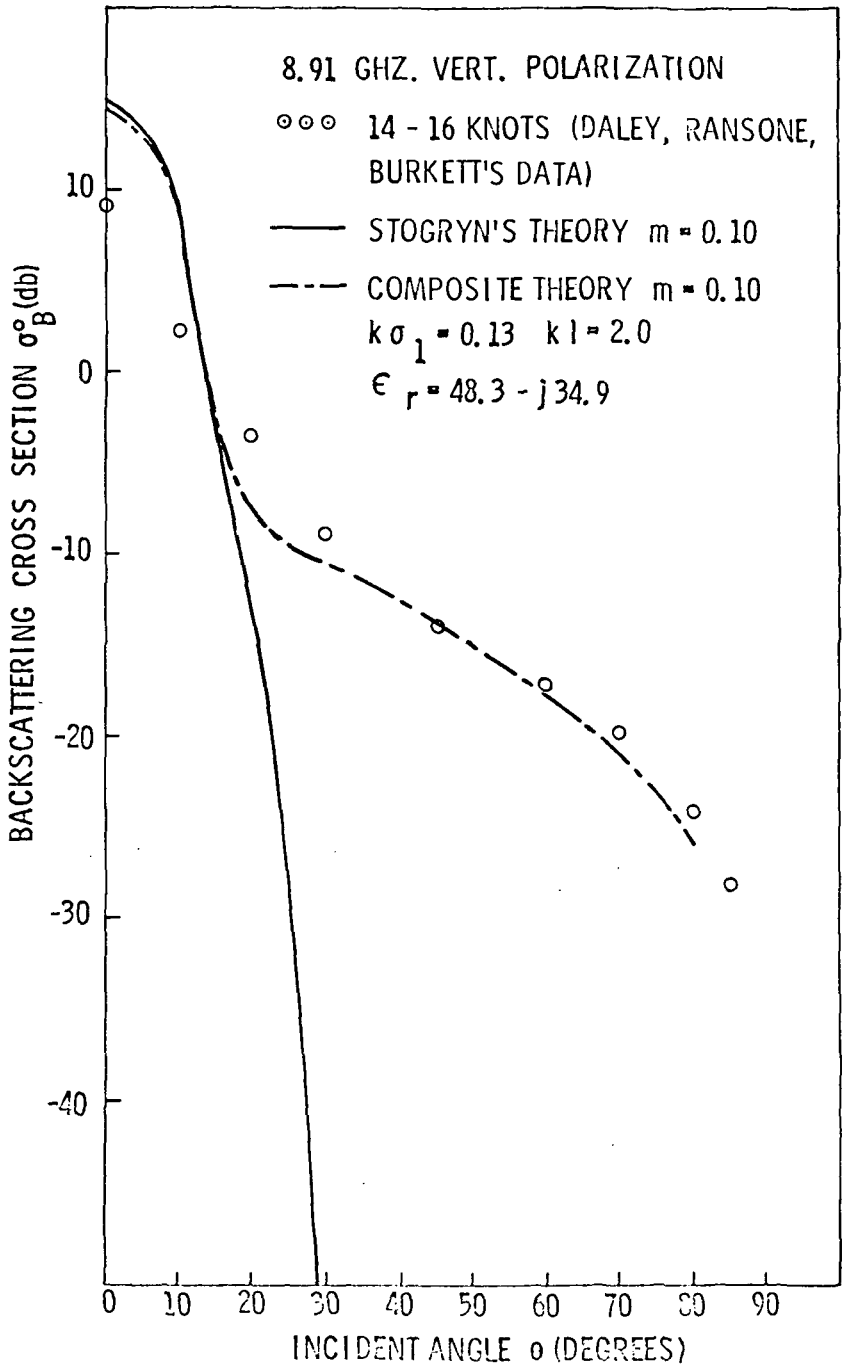

Figure 7. Comparison of computed and measured backscattering cross-section.

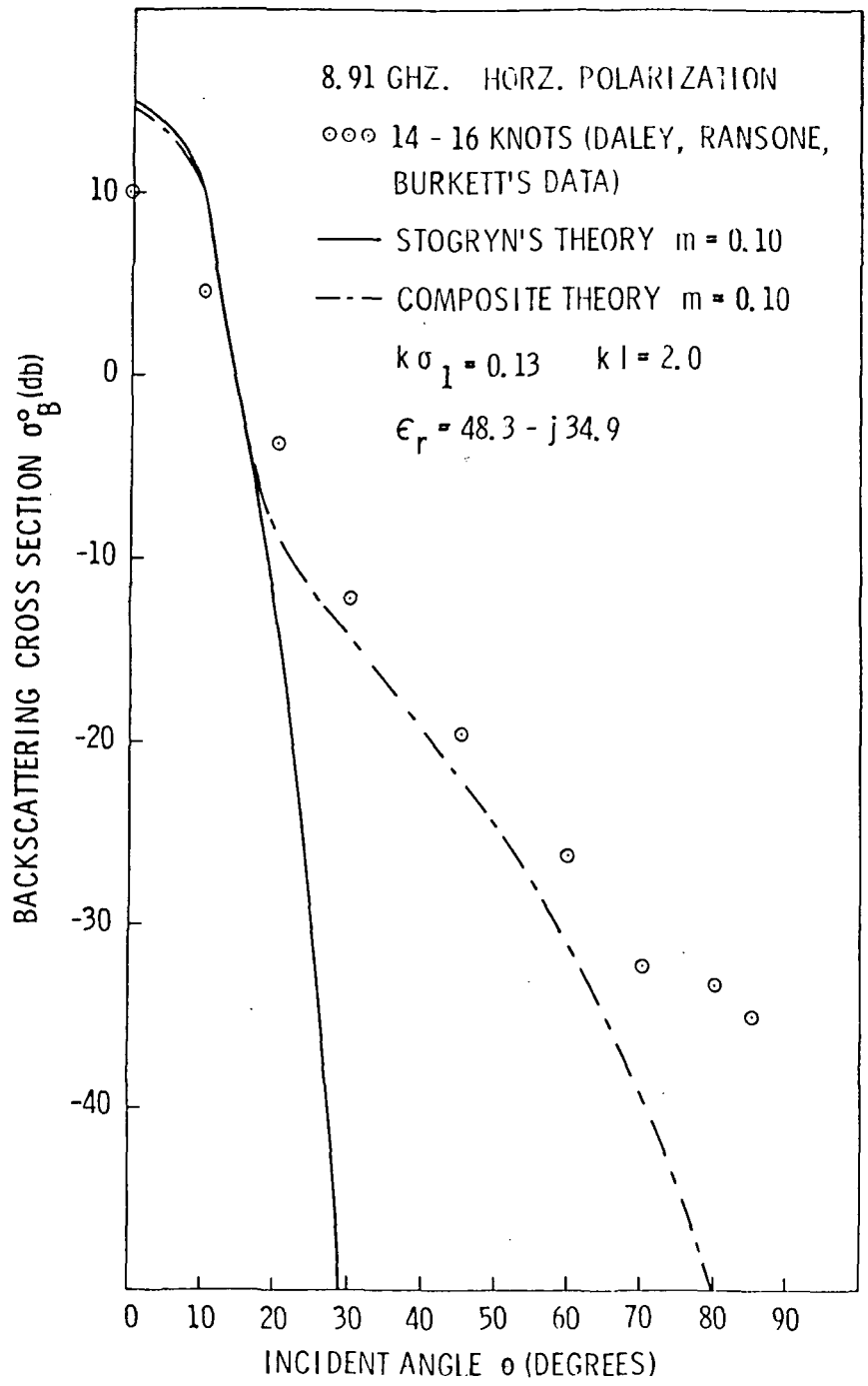

Figure 8. Comparison of computed and measured backscattering cross-section.

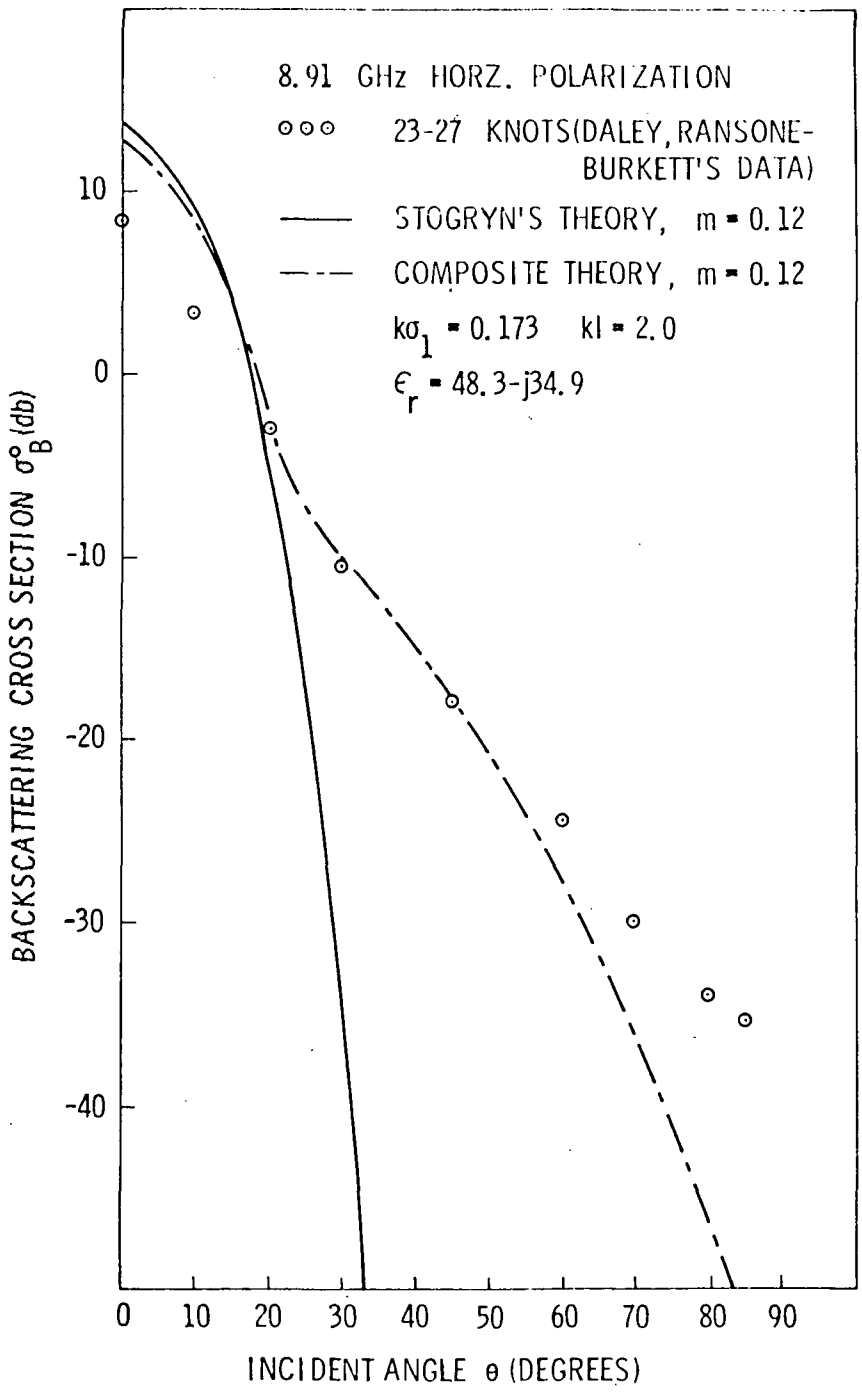

Figure 9. Comparison of computed and measured backscattering cross-section.

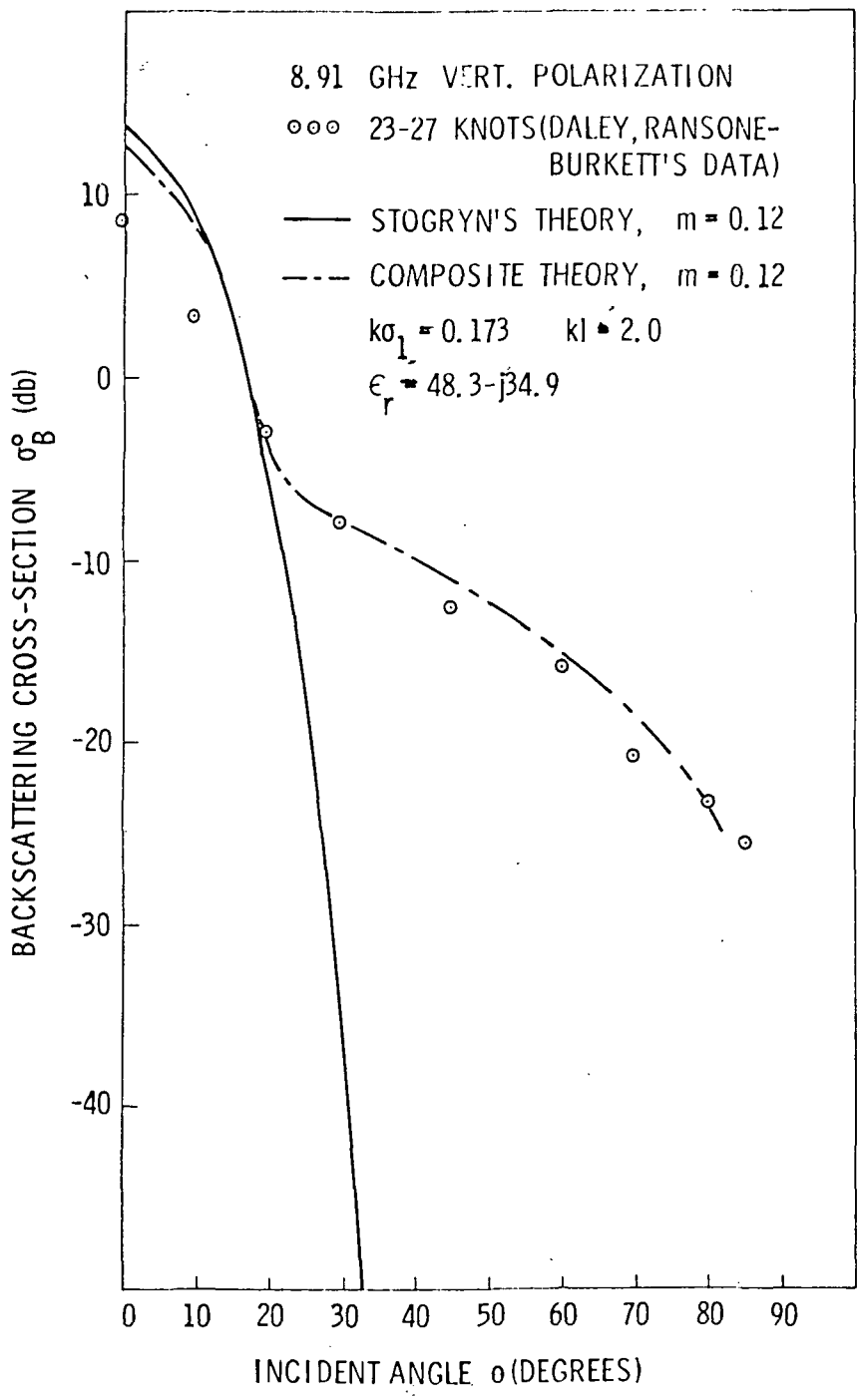

Figure 10. Comparison of computed and measured backscattering cross-section.

REFERENCES

[1] Nordberg, W., J. Conaway and P. Thaddeus, "Microwave Observations of Sea State From Aircraft," Quarterly Journal of the Royal Meteorological Society, vol. 95, pp. 408-413, 1969.

[2] Nordberg, W., J. Conaway, D. B. Ross, T. Wilhert, "Measurement of Microwave Emission from a Foam Covered Wind Driven Sea," Goddard Space Flight Center, X-650-70-384, October 1970 (Submitted to Journal of Atmospheric Sciences).

[3] Ross, D. B., V. J. Cardone, J. W. Conaway, Jr., "Laser and Microwave Observation of Sea-Surface Condition for Fetch Limited 17-25 m/s Winds," IEEE Transactions, vol. GE-8, no. 4, pp. 326-336, October 1970.

[4] Hollinger, J. P., "Passive Microwave Measurements of the Sea Surface," Journal of Geophysical Research, vol. 75, no. 27, pp. 5209-5213, September 1970.

[5] Hollinger, J. P., "Passive Microwave Measurements of Sea Surface Roughness," IEEE Transactions, vol. GE 9, no. 3, pp. 165-169, July 1971.

[6] Stogryn, A., "The Apparent Temperature of the Sea at Microwave Frequencies," IEEE Transactions on Antennas and Propagation, vol. AP-15, no. 2, pp. 278-286, March 1967.

[7] Cox, C. and W. Munk, "Statistics of the Sea Surface Derived from Sun Glitter," Journal of Marine Research, vol. 13, no. 2, pp. 198-227, February 1954.

[8] Semyonov, B., "Approximate Computation of Scattering of Electromagnetic Waves by Rough Surface Contours," Radio Engineering and Electronic Phys., vol. 11, pp. 1179-1187, 1966.

[9] Hollinger, J. P., Private Communication.

[10] Saxton, J. A. and J. A. Lane, "Electrical Properties of Sea Water," Wireless Engr., vol. 29, p. 269, October 1952.

[11] Sutherland, A. J., "Spectral Measurements and Growth Rates of Wind-Generated Water Waves," Stanford University, Dept. of Civil Engineering, Technical Report 84, August 1967.

[12] Peake, W. H., "Interaction of Electromagnetic Waves with Some Natural Surfaces," IRE Transaction, vol. AP-7, Special Supplement, pp. S324-S329, December 1959.

[13] Rice, D. O., "Reflection of Electromagnetic Waves from Slightly Rough Surfaces," Communications in Pure and Applied Mathematics," vol. 4, pp. 361-378, February 1951.

[14] Fung, A. K., "Theory of Cross-Polarized Power Returned From a Random Surface," Appl. Sci. Res. 18, pp. 50-60, August 1967.

[15] Stogryn, A., "Electromagnetic Scattering From Rough, Finitely Conducting Surfaces," Radio Science , vol. 2, (New Series), no. 4, pp. 415-428.

[16] Valenzuela, G. R., "Depolarization of EM Waves by Slightly Rough Surfaces," IEEE Transactions on Antennas and Propagation, vol. AP-15, no. 4, pp. 552-557, July 1967.

[17] Barrick, D. E., and W. H. Peake, "Scattering from Surfaces with Different Roughness Scales: Analysis and Interpretation," Res. Rep. BAT-197A-10-3, Battelle Memorial Institute, Columbus Laboratories, Nov. 1, 1967.

[18] Pierson, W. J., Jr., "A Proposed Vector Wave Number Spectrum for a Study of Radar Sea Return, Microwave Observations of the Sea," NASA/NAVY Review, SP-152, pp. 251-282.

[19] Phillips, O. M., "The Dynamics of the Upper Ocean," Cambridge University Press, London, p. 120, 1966.

[20] Pierson, W. J., Jr., Private Communication.

[21] Cardone, V. J., "Specification of the Wind Distribution in the Marine Boundary Layer for Wave Forecasting," Ph. D. Thesis, New York University, Geophysical Science Laboratory, Technical Report 69-1, December 1969.

[22] Daley, J. C., J. T. Ransome, Jr., and J. A. Burkett, "Radar Sea Return — JOSS I," Naval Research Laboratory, Report No. 7268, May 1971.

[23] Valenzuela, G. R., M. B. Laina and J. C. Daley, "Ocean Spectra for High Frequency Waves from Airborne Radar Measurements," Journal of Marine Research, vol. 29, no. 2, May 1971.

[24] Claassen, J. P. and H. S. Fung, "The Wind Response of Radar Sea Returns and Its Implication on Wave Spectral Growth," University of Kansas Center for Research, Inc., Technical Report 186-5, September 1971. (Available upon Request)

"The aeronautical and space activities of the United States shall be conducted so as to contribute . . . to the expansion of human knowledge of phenomena in the atmosphere and space. The Administration shall provide for the widest practicable and appropriate dissemination of information concerning its activities and the results thereof."

—NATIONAL AERONAUTICS AND SPACE ACT OF 1958

NASA SCIENTIFIC AND TECHNICAL PUBLICATIONS

TECHNICAL REPORTS: Scientific and technical information considered important, complete, and a lasting contribution to existing knowledge.

TECHNICAL NOTES: Information less broad in scope but nevertheless of importance as a contribution to existing knowledge.

TECHNICAL MEMORANDUMS: Information receiving limited distribution because of preliminary data, security classification, or other reasons. Also includes conference proceedings with either limited or unlimited distribution.

CONTRACTOR REPORTS: Scientific and technical information generated under a NASA contract or grant and considered an important contribution to existing knowledge.

TECHNICAL TRANSLATIONS: Information published in a foreign language considered to merit NASA distribution in English.

SPECIAL PUBLICATIONS: Information derived from or of value to NASA activities. Publications include final reports of major projects, monographs, data compilations, handbooks, sourcebooks, and special bibliographies.

TECHNOLOGY UTILIZATION PUBLICATIONS: Information on technology used by NASA that may be of particular interest in commercial and other non-aerospace applications. Publications include Tech Briefs, Technology Utilization Reports and Technology Surveys.

Details on the availability of these publications may be obtained from:

SCIENTIFIC AND TECHNICAL INFORMATION OFFICE

NATIONAL AERONAUTICS AND SPACE ADMINISTRATION

Washington, D.C. 20546